IOP Publishing Physica Scripta
Phys. Scr. **76** (2007) 397–409 doi:10.1088/0031-8949/76/4/020

In-depth analysis of Coulomb–Volkov approaches to ionization and excitation by laser pulses

Guichard R, Bachau H, Cormier E, Gayet R and Rodriguez V D[1]

Centre Lasers Intenses et Applications, Université Bordeaux 1, 351 Cours de la Libération, 33405 Talence Cedex, France

Received 15 June 2007
Accepted for publication 9 August 2007
Published 18 September 2007
Online at stacks.iop.org/PhysScr/76/397

Abstract
In perturbation conditions, above-threshold ionization spectra produced in the interaction of atoms with femtosecond short-wavelength laser pulses are well predicted by a theoretical approach called $CV2^-$, which is based on Coulomb–Volkov-type states. However, when resonant intermediate states play a significant role in a multiphoton transition, the $CV2^-$ transition amplitude does not take their influence into account. In a previous paper, this influence has been introduced separately as a series of additional sequential processes interfering with the direct process. To give more credit to this procedure, called modified $CV2^-$ ($MCV2^-$), a perturbation expansion of the standard $CV2^-$ transition amplitude is compared here to the standard time-dependent perturbation series and the strong field approximation. It is shown that the $CV2^-$ transition amplitude consists merely in a simultaneous absorption of all photons involved in the transition, thus avoiding all intermediate resonant state influence. The present analysis supports the $MCV2^-$ procedure that consists in introducing explicitly the other quantum paths, which contribute significantly to ionization, such as passing through intermediate resonances. Further, this analysis permits to show that multiphoton excitation may be addressed by a Coulomb-Volkov approach akin to $MCV2^-$.

PACS numbers: 42.50.Hz, 32.80.Rm, 32.80.Fb

1. Introduction

New experimental and theoretical findings recently focused on the strengths and weaknesses of the widely known strong field approximation (SFA) [1, 2] for above-threshold ionization (ATI) phenomena by long wavelength laser fields. On the one hand, it has been found that an SFA based approach explains very well the multiphoton detachment of electrons from negative ions [3]. On the other hand, SFA has provided a theoretical framework to understand qualitatively ATI from neutral atoms [4]. Quite recently, it was found that SFA predictions for the electron momentum distributions do not show the experimentally observed cusp at zero electron momentum, exhibiting instead a smooth behavior [5]. Further, to agree with the experiments, the authors of [5] had to introduce a Coulomb–Volkov final wavefunction in SFA [6]. This drawback of SFA has been invoked to explain the discrepancy between the low energy spectra predicted by SFA and a numerical solution of the Schrödinger equation [7]. Again, SFA failure has been attributed in the later case to the omission of the long-range character of the Coulomb potential in the final state.

If SFA and the CV approximation have been widely studied in the context of infrared lasers (IR), much less is known in the UV or X range. It is the aim of this paper to investigate this aspect. In fact, in previous publications [8, 9], it was established that a simple theoretical approach called $CV2^-$, which is based on Coulomb-Volkov-type(CV) states [10], could supply reliable predictions of atomic ionization by extreme ultraviolet laser pulses down to the subfemtosecond regime. For any field parameter, it was shown that $CV2^-$ provides accurate energy distributions of ejected electrons, including many ATI peaks, as long as the two following conditions are simultaneously

[1] Permanent address: Departamento de Física, Facultad de Ciencias Exactas y Naturales, Universidad de Buenos Aires, 1428 Buenos Aires, Argentina.

fulfilled: (i) the photon energy is greater than or equal to the ionization potential I_P and (ii) the ionization process is not saturated. The condition (i) restricts CV2$^-$ application to VUV laser pulses (e.g. high-enough harmonics of Ti-Sapphire lasers), while the condition (ii) limits CV2$^-$ application to laser intensities compatible with the perturbation regime. Therefore, further systematic studies have been conducted to extend the field of application of CV approaches to laser pulse-induced transitions.

On the one hand, keeping condition (i), a renormalization procedure, which takes into account the depletion of the initial state in the course of irradiation, has been introduced successfully [11]. This new approach, called RCV2$^-$ (renormalized CV2$^-$), permits to get rid of condition (ii), thus opening the way to application of Coulomb-Volkov approaches to ionization by laser pulses with $\hbar\omega \geqslant I_P$ whatever the laser intensity.

On the other hand, keeping condition (ii), i.e. in perturbation conditions, the application of CV2$^-$ has been extended to higher laser wavelengths [12]. It was achieved by introducing a 'trial initial state' that encompasses the actual initial state itself and all intermediate bound states that can be excited during the pulse. The new approach has been first restricted to laser wavelengths such that, owing to the spectral width of the laser pulse, only a few intermediate bound states $|\gamma\rangle$ can be excited in single-photon absorption [12]. In this particular case, the time-dependent coefficient of an intermediate state $|\gamma\rangle$ is simply given by the first-order perturbation amplitude of transition from the initial state to $|\gamma\rangle$. In its present state, this procedure, which has been called modified CV2$^-$ (MCV2$^-$), can address ionization by photons whose energy may be as small as half the target ionization potential, i.e. by low harmonics that are currently generated using femtosecond Ti-Sapphire laser pulses [13].

To better understand why standard CV2$^-$ predictions of ATI peaks are so accurate in perturbation conditions, it appears interesting to compare CV2$^-$ to the standard Born perturbation series (BPS). Indeed, the nth order of BPS, which corresponds to an n-photon transition, provides good predictions of the corresponding ATI peak as long as perturbation conditions prevail. Hereafter, it is shown that the original approach CV2$^-$ discards quantum paths connected to intermediate resonant states. This analysis bears out the procedure leading to the approach MCV2$^-$ [12]. Although it is made with hydrogen-like targets, this analysis may be generalized to any target. Finally, the approximations that are studied here are compared to calculations made without approximation. These later calculations, hereafter referred to as TDSE, are based on the resolution of the time-dependent Schrödinger equation [14]. The paper is organized as follows.

In section 2, the standard Coulomb-Volkov theory CV2$^-$ for transitions induced by short laser pulses in the perturbation regime is briefly reviewed. Its connection with the length-gauge version of the SFA is addressed.

In section 3, the CV2$^-$ transition amplitude is expanded in a series of increasing perturbation orders. Then, the CV2$^-$ perturbation series is compared to the BPS.

As a support of the preceding study, new TDSE results are presented in section 4 to verify previous predictions made by CV2$^-$ and MCV2$^-$ for atom ionization in perturbation conditions [9, 12]. As expected, according to section 3, CV2$^-$ electron spectra are extremely accurate for $\hbar\omega > I_P$ [9], while the adapted treatment MCV2$^-$ is required at smaller laser frequencies [12]. An improved CV2$^-$ spectrum is obtained by means of a fast and accurate time-integration technique already used in [12]. The essential role of the Coulomb factor is illustrated by comparing CV2$^-$ with calculations performed within SFA. Further, it is shown that, the electron spectrum background is quasi identical to the background predicted by the first-order of BPS (Born approximation). In appendix A, this background is shown to strongly depend on the characteristics of the pulse (mainly the Fourier transform of the laser electric field envelop). Some examples of the background dependence on the pulse duration are given in appendix A. The main features of the time-integration technique are given in appendix B.

Appendix C is a complement of section 3.2. The CV2$^-$ amplitude is first transformed into a perturbation series. Then, it is compared to the amplitude calculated within the second-order of the BPS.

In section 5, one analyzes the laser-induced excitation probability as a function of the laser frequency. As for ionization, it is shown that differences between CV2$^-$ predictions and TDSE may be elucidated according to the analysis made in section 3.

Conclusions and perspectives are drawn in section 6.

Atomic units are used throughout unless otherwise stated.

2. Derivation of the transition amplitude CV2$^-$

In nonrelativistic conditions, the wavefunction $\Psi(\vec{r}, t)$ of a hydrogen-like atom interacting with an external electromagnetic field $\vec{F}(\vec{r}, t)$, that is assumed to be almost uniform in a large region around the atom at a given time t (dipole approximation), is given by the time-dependent Schrödinger equation:

$$\mathrm{i}\frac{\partial \Psi(\vec{r}, t)}{\partial t} = [H_0 + V(t)]\ \Psi(\vec{r}, t), \tag{1a}$$

$$H_0 = -\frac{\nabla^2}{2} - \frac{Z}{r}, \tag{1b}$$

$$V(t) = \vec{r} \cdot \vec{F}(t), \tag{1c}$$

where $\vec{r}$ gives the position of the electron with respect to the nucleus identified with the centre-of-mass; Z is the nuclear charge and $\vec{F}(t)$ is the external field at the atom. The field-free initial and final states are $\phi_i(\vec{r}, t)$ and $\phi_f^-(\vec{r}, t)$, respectively:

$$\phi_i(\vec{r}, t) = \varphi_i(\vec{r})\ \exp(-\mathrm{i}\varepsilon_i t), \tag{2a}$$

$$\phi_f^-(\vec{r}, t) = \varphi_f^-(\vec{r})\ \exp\left(-\mathrm{i}\varepsilon_f t\right), \tag{2b}$$

where $\varphi_i(\vec{r})$ and $\varphi_f^-(\vec{r})$ are eigenstates of the field-free Hamiltonian H_0; ε_i (resp. ε_f) is the eigenenergy of the initial (resp. final) unperturbed stationary state $\varphi_i(\vec{r})$, (resp. $\varphi_f^-(\vec{r})$). In $\varphi_f^-(\vec{r})$, the subscript '$-$' indicates that the unperturbed final state must be featured by an *ingoing* regular Coulomb

wavefunction when the final state lies in the continuum. In this later case, $\varphi_f^-(\vec{r})$ is explicitly:

$$\varphi_f^-(\vec{r}) = (2\pi)^{-3/2} \exp\left(+\frac{\pi\nu}{2}\right) \Gamma(1+\mathrm{i}\nu) \exp(\mathrm{i}\vec{k}\cdot\vec{r}) \times {}_1F_1(-\mathrm{i}\nu; 1; -\mathrm{i}kr - \mathrm{i}\vec{k}\cdot\vec{r}), \quad (3)$$

where $\vec{k}$ is the electron momentum and $\nu = 1/k$. $\varphi_f^-(\vec{r})$ is normalized to $\delta(\vec{k}-\vec{k}')$ and its eigenenergy is $\varepsilon_f = k^2/2$.

As to the electric field of the laser, it is derived from a vector potential $\vec{A}(t)$; thus one has:

$$\vec{F}(t) = -\frac{\partial \vec{A}(t)}{\partial t}. \quad (4)$$

Therefore, the general form of $\vec{A}(t)$ may be written as:

$$\vec{A}(t) - \vec{A}(t_0) = -\int_{t_0}^{t} \mathrm{d}t' \vec{F}(t'), \quad (5)$$

where t_0 is arbitrary. In what follows, we restrict our study to the interaction of a hydrogen atom with a linearly polarized laser pulse in the dipole approximation. Thus, in the vicinity of the atom, the external laser field may be written as:

$$\vec{F}(t) = F_{\mathrm{M}}\,\vec{\lambda}\,\sin(\omega t + \varphi)\;\; f_\tau(t), \quad (6)$$

where F_{M} is the maximum value of the electric field and $\vec{\lambda}$ is a unitary vector that gives the direction of the linear polarization. $f_\tau(t)$ is the modulation in time of the maximum value of the electric field. This time-envelope, which defines the shape of the pulse, satisfies the following conditions:

$$\begin{cases} 0 \leqslant f_\tau(t) \leqslant 1, \\ f_\tau(t) \neq 0 \qquad \text{only when } t \in [0\,,\,\tau]\,, \end{cases} \quad (7)$$

where τ is the total duration of the pulse. As in previous studies, calculations reported in section 4 are performed with a pulse shape that is featured through a sine-square envelope. Thus one has here:

$$f_\tau(t) = \sin^2\left(\frac{\pi t}{\tau}\right), \quad (8)$$

and the pulse is made symmetric with respect to $t = \tau/2$ by fixing $\varphi = (\pi/2) - \omega(\tau/2)$ (in fact, the phase φ matters little when many oscillations are performed during the pulse).

With both, the final state $\phi_f^-(\vec{r},t)$ and the laser field, one builds the final Coulomb-Volkov wavefunction $\chi_f^-(\vec{r},t)$ that must be an *ingoing* Coulomb-Volkov wavefunction when $\varepsilon_f > 0$. According to [8, 9], one has:

$$\begin{cases} \chi_f^- = \phi_f^-(\vec{r},t) L^-(\vec{r},t), \\ L^-(\vec{r},t) = \exp\left\{\mathrm{i}\vec{A}^-(t)\cdot\vec{r} - \mathrm{i}\vec{k}\cdot\displaystyle\int_\tau^t \mathrm{d}t'\vec{A}^-(t') \right. \\ \qquad\qquad \left. -\dfrac{\mathrm{i}}{2}\displaystyle\int_\tau^t \mathrm{d}t'\vec{A}^{-2}(t')\right\}, \end{cases} \quad (9)$$

where $\vec{A}^-(t)$ is the variation of $\vec{A}(t)$ that must be considered in a time-reversal picture. The last term in the argument of $L^-(\vec{r},t)$ is related to the ponderomotive shift U_{p} [11]. Owing to the values of the intensity and wavelength used here, U_{p} is small. Therefore, it does not play any significant role and it can be omitted. We have verified that in actual calculations, the expression of $L^-(\vec{r},t)$ to be introduced in transition amplitudes can be simplified to [12]:

$$L^-(\vec{r},t) = \exp\left\{\mathrm{i}\vec{A}^-(t)\cdot\vec{r} - \mathrm{i}\vec{k}\cdot\int_\tau^t \mathrm{d}t'\vec{A}^-(t')\right\}. \quad (10)$$

If the final state is a bound state, i.e. a non-traveling state, the average velocity is zero and thus one must set $\vec{k} = \vec{0}$.

In the Schrödinger picture, the transition amplitude from the state i before interaction to the final state f after interaction, is:

$$T_{fi} = \langle \Psi_f^-(t) | \Psi_i^+(t) \rangle, \quad (11)$$

where t may be any time; $\Psi_f^-(\vec{r},t)$ and $\Psi_i^+(\vec{r},t)$ are the exact solutions of the equation (1) subject to the asymptotic conditions:

$$\Psi_f^-(\vec{r},t) \underset{t\to+\infty}{\longrightarrow} \phi_f^-(\vec{r},t), \quad (12a)$$

$$\Psi_i^+(\vec{r},t) \underset{t\to-\infty}{\longrightarrow} \phi_i(\vec{r},t). \quad (12b)$$

The so-called *prior* form of T_{fi}, which leads to the approach CV2$^-$ [8, 9], is:

$$T_{fi}^- = \lim_{t\to-\infty} \langle \Psi_f^-(t) \,|\, \Psi_i^+(t) \rangle = \lim_{t\to-\infty} \langle \Psi_f^-(t) \;|\phi_i(t)\rangle. \quad (13)$$

After a standard easy algebra, using (1*a*) and (12*a* and *b*), and keeping in mind that $\phi_i(\vec{r},t)$ and $\phi_f^-(\vec{r},t)$ are orthogonal, the expression (13) may be transformed into:

$$T_{fi}^- = -\mathrm{i}\int_0^\tau \mathrm{d}t \langle \Psi_f^-(t) | V(t) | \phi_i(t) \rangle. \quad (14)$$

The standard approach CV2$^-$ consists in substituting the Coulomb–Volkov wavefunction $\chi_f^-(\vec{r},t)$ for $\Psi_f^-(\vec{r},t)$ in (14), i.e.:

$$T_{fi}^{\mathrm{CV2}^-} = -\mathrm{i}\int_0^\tau \mathrm{d}t \langle \chi_f^-(t) | V(t) | \phi_i(t) \rangle. \quad (15)$$

Then, according to expressions (2a), (2b), (9) and (10) one gets:

$$T_{fi}^{\mathrm{CV2}^-} = -\mathrm{i}\int_0^\tau \mathrm{d}t \exp\left\{\mathrm{i}(\varepsilon_f - \varepsilon_i)t + \mathrm{i}\vec{k}\cdot\int_\tau^t \mathrm{d}t'\vec{A}^-(t')\right\} \times \int \mathrm{d}\vec{r}\,\varphi_f^{-*}(\vec{r}) \exp\left\{-\mathrm{i}\vec{A}^-(t)\cdot\vec{r}\right\} \vec{r}\cdot\vec{F}(t)\,\varphi_i(\vec{r}). \quad (16)$$

Again, let us remind that $\vec{k} = \vec{0}$ if the final state is a bound one. We can relate here the CV2$^-$ transition amplitude to the strong field approximation's one in the length gauge. The latter is obtained from the former by just setting the nuclear charge in the final wavefunction to zero.

Then, one introduces the useful functions:

$$h^-(t) = \mathrm{i}(\varepsilon_f - \varepsilon_i) + \mathrm{i}\vec{k}\cdot\vec{A}^-(t), \quad (17)$$

$$f^-(t) = \exp\left\{\int_\tau^t \mathrm{d}t' h^-(t')\right\}, \quad (18)$$

$$g^-(t) = \int \mathrm{d}\vec{r}\,\varphi_f^{-*}(\vec{r}) \exp\left\{-\mathrm{i}\vec{A}^-(t)\cdot\vec{r}\right\} \varphi_i(\vec{r}), \quad (19)$$

where $\varepsilon_f = k^2/2$ if the final state lies in the continuum. Using a standard procedure [15], one gets an analytical expression for $g^-(t)$. With the expressions (6) and (8) of the external field $\vec{F}(t)$, the functions $h^-(t)$ and $f^-(t)$ may also be calculated analytically. If the form of $\vec{F}(t)$ is too complicated, it is not difficult to perform accurate numerical time integrations (see appendix B). Integrating by parts and bearing in mind that $\vec{A}^-(\tau) = \vec{0}$, one obtains [9]:

$$T_{fi}^{\mathrm{CV2}^-} = f^-(0)\, g^-(0) - \int_0^\tau \mathrm{d}t\, h^-(t)\; f^-(t)\, g^-(t). \qquad (20)$$

It is worth noting that the first term of the rhs in (20) is zero for a genuine laser pulse since one has also $\vec{A}^-(0) = \vec{0}$ (no direct electric field). Therefore, a simple numerical integration over the pulse duration is necessary to know $T_{fi}^{\mathrm{CV2}^-}$. Here, we use now an effective and accurate integration procedure that is sketched in appendix B.

Then, whatever approximation used, the transition probability is given by $|T_{fi}|^2$. If the final state lies in the continuum, the angular and energy distribution of ejected electrons is given by the general expression:

$$\frac{\partial^2 P_{fi}}{\partial E_k \partial \Omega_k} = k|T_{fi}|^2, \qquad (21)$$

where E_k and Ω_k are the energy and the direction corresponding to the momentum $\vec{k}$ of the ejected electron. Integrating with respect to Ω_k gives the energy distribution $\partial P_{fi}/\partial E_k$ and a further integration with respect to E_k gives the total probability P_{fi} to ionize an atom with one pulse. For $\hbar\omega > I_{\mathrm{P}}$, it was shown [9] that accurate predictions are made by CV2$^-$ as long as $P_{fi}^{\mathrm{CV2}^-}$ does not exceed 20%.

3. Perturbation series

3.1. BPS

In the interaction picture, the Born perturbation expansion of the T-matrix transition element is obtained by iterating p times the integral equation of the evolution operator (see, e.g. [17]). It can be written as:

$$T_{fi} = \sum_{p=1} T_{fi}^{(p)}. \qquad (22)$$

As usual, post and prior forms to any order of this expansion are identical. The pth order of BPS is the well-known formula:

$$T_{fi}^{(p)} = (-\mathrm{i})^p \sum_{j_1}\sum_{j_2}\cdots\sum_{j_p}\int_0^\tau \mathrm{d}t_1 \int_0^{t_1}\mathrm{d}t_2 \cdots \int_0^{t_{p-1}}\mathrm{d}t_p$$
$$\times \left\langle \phi_f^-(t_1)\right|\; V(t_1)\; \left|\phi_{j_1}(t_1)\right\rangle\left\langle\phi_{j_1}(t_2)\right|\; V(t_2)\left|\phi_{j_2}(t_2)\right\rangle$$
$$\cdots \left\langle\phi_{j_{p-1}}(t_p)\right|\; V(t_p)\; \left|\phi_i(t_p)\right\rangle. \qquad (23)$$

This pth order is the amplitude to absorb p-photons during the irradiation. The first Born approximation, hereafter referred to as B1, which corresponds to $p = 1$, can also be obtained by substituting $\phi_f^-(\vec{r}, t)$ for $\Psi_f^-(\vec{r}, t)$ in (14), thus leading to:

$$T_{fi}^{\mathrm{B1}} = -\mathrm{i}\int_0^\tau \mathrm{d}t \langle\phi_f^-(t)|V(t)|\phi_i(t)\rangle. \qquad (24)$$

Under perturbation conditions, the $(p+1)$th term should be smaller than the corresponding pth one. Thus, one expects the spectrum to be dominated by B1, except in the neighborhood of a N-photon absorption resonance, i.e. when one has: $\varepsilon_f - \varepsilon_i \simeq N\omega$. In this case, the multiple time-integration term becomes large and a characteristic peak structure emerges over the background that is given by the lowest nonzero perturbation term. For ionization, this background is actually given by B1. However, when one considers an increasing number of absorbed photons for a finite pulse duration, the corresponding ATI peak will finally disappear below the background.

3.2. Perturbation series of CV2$^-$

To investigate what processes are actually contained in a standard CV2$^-$ approach, the amplitude (23) is compared here with the corresponding order of a suitable perturbation series of CV2$^-$. First, let us write the perturbation in the form:

$$\vec{F}(t) = \alpha\, \vec{F}_0(t) = \alpha\, F_0\, \vec{\lambda}\, \sin(\omega t + \varphi)\; f_\tau(t), \qquad (25)$$

where F_0 is now the value of the electric field experienced by the electron on the first Bohr orbit of the target. Thus, $\alpha = F_{\mathrm{M}}/F_0$, i.e. α is the ratio of the laser field amplitude to the average nuclear Coulomb field in the entrance channel. Thus, perturbation conditions imply $\alpha \ll 1$. To simplify the notation, one defines:

$$\vec{A}_0(t) = \vec{A}_0^+(t) = -\int_0^t \vec{F}_0(t)\,\mathrm{d}t; \quad \vec{A}_0^-(t) = -\int_\tau^t \vec{F}_0(t)\,\mathrm{d}t. \qquad (26)$$

Since one has $\vec{A}_0(\tau) = \vec{0}$, for a true laser pulse, it is readily seen that $\vec{A}_0^-(t) = \vec{A}_0(t)$. Then, the transition amplitude (16) reads:

$$T_{fi}^{\mathrm{CV2}^-} = -\mathrm{i}\int_0^\tau \mathrm{d}t \exp\left\{\mathrm{i}(\varepsilon_f - \varepsilon_i)t + \mathrm{i}\vec{k}\cdot\int_\tau^t \mathrm{d}t'\alpha\vec{A}^-(t')\right\}$$
$$\times \int \mathrm{d}\vec{r}\;\varphi_f^{-*}(\vec{r})\exp\left\{-\mathrm{i}\alpha\vec{A}_0^-(t)\cdot\vec{r}\right\}\alpha\vec{r}\cdot\vec{F}_0(t)\varphi_i(\vec{r}). \qquad (27)$$

To expand (27) in a perturbation series of the parameter α, it is written more conveniently:

$$T_{fi}^{\mathrm{CV2}^-} = -\mathrm{i}\int_0^\tau \mathrm{d}t \exp\left[\mathrm{i}(\varepsilon_f - \varepsilon_i)t\right]\int \mathrm{d}\vec{r}\varphi_f^{-*}(\vec{r})$$
$$\times \exp\left\{-\mathrm{i}\alpha\left[\vec{A}_0^-(t)\cdot\vec{r} - \vec{k}\cdot\int_\tau^t \mathrm{d}t'\,\vec{A}_0^-(t')\right]\right\}\alpha\vec{r}\cdot\vec{F}_0(t)\,\varphi_i(\vec{r}). \qquad (28)$$

Then, expanding the exponential function into a Taylor series leads to:

$$T_{fi}^{\mathrm{CV2}^-} = -\mathrm{i}\int_0^\tau \mathrm{d}t \exp\left\{\mathrm{i}(\varepsilon_f - \varepsilon_i)t\right\}\int \mathrm{d}\vec{r}\,\varphi_f^{-*}(\vec{r})$$
$$\times\left\{1 + \sum_{p=1}^{\infty}\frac{(-\mathrm{i})^p\alpha^p}{p!}\left[\vec{r}\cdot\vec{A}_0^-(t) - \vec{k}\cdot\int_\tau^t \mathrm{d}t'\vec{A}_0^-(t')\right]^p\right\}$$
$$\times\,\alpha\vec{r}\cdot\vec{F}_0(t)\varphi_i(\vec{r}). \qquad (29)$$

The first-order term (linear in α) is nothing but B1 (24). To better analyze subsequent orders, let us study the second-order

term in $\alpha^2 (p = 1)$. It is:

$$T_{fi}^{\mathrm{CV2^-}} = (-\mathrm{i}\alpha)^2 \int_0^\tau \mathrm{d}t \exp\left\{\mathrm{i}(\varepsilon_f - \varepsilon_i)t\right\} \int \mathrm{d}\vec{r}\, \varphi_f^{-*}(\vec{r}) \times \left\{\vec{r}\cdot\vec{A}_0^-(t) - \vec{k}\cdot\int_\tau^t \mathrm{d}t'\, \vec{A}_0^-(t')\right\} \vec{r}\cdot\vec{F}_0(t)\varphi_i(\vec{r}). \quad (30)$$

Let us first concentrate on the second term of the right-hand side of (30). It is connected to the electron displacement during the interaction. This term is a second-order contribution to the first-order term (one-photon transition). In fact, summing all subsequent contributions to the first order that appear in (29), it is easy to see that the one-photon transition amplitude reads:

$$T_{fi}^{\mathrm{CV2^-}\,(1)} = -\mathrm{i}\int_0^\tau \mathrm{d}t\, \exp\left\{\mathrm{i}\left(\varepsilon_f - \varepsilon_i\right)t + \mathrm{i}\,\alpha\vec{k}\cdot\int_\tau^t \mathrm{d}t'\, \vec{A}_0^-(t')\right\} \times \int \mathrm{d}\vec{r}\, \varphi_f^{-*}(\vec{r})\, \alpha\, \vec{r}\cdot\vec{F}_0(t)\, \varphi_i(\vec{r}). \quad (31)$$

When the final state is a bound one, i.e. a non-traveling state, one must set $\vec{k}$ to $\vec{0}$, thus avoiding any electron displacement contribution. If the final state is in the continuum, the electron displacement term in the argument of the exponential in (31) generally does not vanish. However, this term may be neglected since it is a first-order correction compared to $\mathrm{i}(\varepsilon_f - \varepsilon_i)t$. Therefore, for $\hbar\omega \geqslant I_\mathrm{P}$ in the perturbation regime, one expects the single-photon ionization peak of the electron spectrum predicted by CV2$^-$ to be almost identical to the peak predicted by the first order of perturbation. Further, it has also been shown in [8] that the influence of the electron displacement on higher-order peaks cannot be neglected. A detailed study of this influence is outside the scope of the present paper that aims at identifying in CV2$^-$ the flaws that prevent this theory from providing reliable predictions of multiphoton ionization when $\hbar\omega < I_\mathrm{P}$.

Indeed, one sees that electron spectra predicted by CV2$^-$ are accurate only when $\hbar\omega > I_\mathrm{P}$ [8, 9, 12]. This observation leads us to conclude that some resonant processes, which must show up when $\hbar\omega < I_\mathrm{P}$, are not taken into account in a standard approach CV2$^-$. Indeed, within the spectral width of the laser pulse, a band of bound states may be excited in this case, thus introducing new quantum paths that interfere with the 'direct' multiphoton ionization process. Although these intermediate bound states appear explicitly in the standard perturbation expansion (23), it is not the case for the CV2$^-$ expansion (29). To investigate the difference, let us come back to the two-photon amplitude (30) deprived of the electron displacement term:

$$T_{fi}^{\mathrm{CV2^-}\,(2)} = (-\mathrm{i}\,\alpha)^2 \int_0^\tau \mathrm{d}t \int \mathrm{d}\vec{r}\, \phi_f^{-*}(\vec{r},t)\vec{r}\cdot\vec{A}_0^-(t)\, \vec{r}\cdot\vec{F}_0(t)\phi_i(\vec{r},t). \quad (32)$$

Substituting $\vec{r}\cdot\vec{F}_0(t)$ for $V(t)$ in the corresponding second-order term of BPS (23), one gets:

$$T_{fi}^{(2)} = (-\mathrm{i}\,\alpha)^2 \int_0^\tau \mathrm{d}t \int_0^t \mathrm{d}t' \int \mathrm{d}\vec{r}\, \phi_f^{-*}(\vec{r},t)\,\vec{r}\cdot\vec{F}_0(t) \times \sum_j \phi_j(\vec{r},t) \int \mathrm{d}\vec{r}'\phi_j^*(\vec{r}',t')\,\vec{r}'\cdot\vec{F}_0(t')\,\phi_i(\vec{r}',t'). \quad (33)$$

We show in appendix C that the equation (32) can be written:

$$T_{fi}^{\mathrm{CV2^-}\,(2)} = (-\mathrm{i}\,\alpha)^2 \int_0^\tau \mathrm{d}t F_0(t) \sum_j D_{fj}(t)\,\tilde{\Gamma}_{ji}(t), \quad (34)$$

where $D_{fj}(t)$ is the dipole matrix element between states j and f (see expression (C.5) in appendix C) and $\tilde{\Gamma}_{ji}(t)$ is:

$$\tilde{\Gamma}_{ji}(t) = \int_0^t \mathrm{d}t'\delta\left(t'-t\right)\, A_0(t')\, D_{ji}(t') = -D_{ji}(t)\int_0^t \mathrm{d}t'\, F_0(t'). \quad (35)$$

While the second order of BPS reads:

$$T_{fi}^{(2)} = (-\mathrm{i}\,\alpha)^2 \int_0^\tau \mathrm{d}t F_0(t) \sum_j D_{fj}(t)\,\Gamma_{ji}(t), \quad (36)$$

with:

$$\Gamma_{ji}(t) = \int_0^t \mathrm{d}t'\, F_0(t')\, D_{ji}(t')\,. \quad (37)$$

The expression (34) has a form similar to (36), except that $\tilde{\Gamma}_{ji}(t)$, as defined in (35), does not include the history of the transition to any intermediate state j from $t' = 0$ to $t' = t$ all along the interaction with the laser field. It is as if any passage by an intermediate state j lasted an infinitesimal time, thus preventing any resonant transition to an intermediate state from taking place. Such a resonant transition is precisely described by the 2nd term in the rhs of expression (C.18), in appendix C.

Now, it is clear that passing through resonant intermediate states is excluded from any CV2$^-$ approach. Therefore, such a quantum path has to be introduced explicitly in CV2 calculations when it is likely to contribute significantly to a laser-induced transition. It was precisely the aim of the MCV2$^-$ approach [12] where it has been shown that combining the 'direct' CV2$^-$ amplitude (16) with the amplitudes of transient intermediate state excitation lead to accurate predictions.

The problem linked with the lack of intermediate resonance is illustrated in the following sections in the case of laser-induced atomic ionization and excitation.

4. CV2$^-$ approach to laser-induced multiphoton ionization of atoms

4.1. Analysis of CV2$^-$ electron spectra

The ionization transition amplitude is given by the expressions (16)–(20). To avoid difficulties in the time integration over the pulse duration, one uses a simple adapted numerical technique, details of which are briefly sketched in appendix B. This technique was used for the first time in [12] in place of a previous integration procedure that showed significant imperfections at rather high laser intensities when the pulse length increases (see figures 3(e) and (f) of paper [9]). Since the new time integration procedure is now used in all CV2$^-$ calculations, it is worth showing how reliable it is. Therefore, a CV2$^-$ electron spectrum corresponding to figure 3(f) in [9] is obtained with the new technique. It is reported on figure 1(b) up to an ejected electron energy

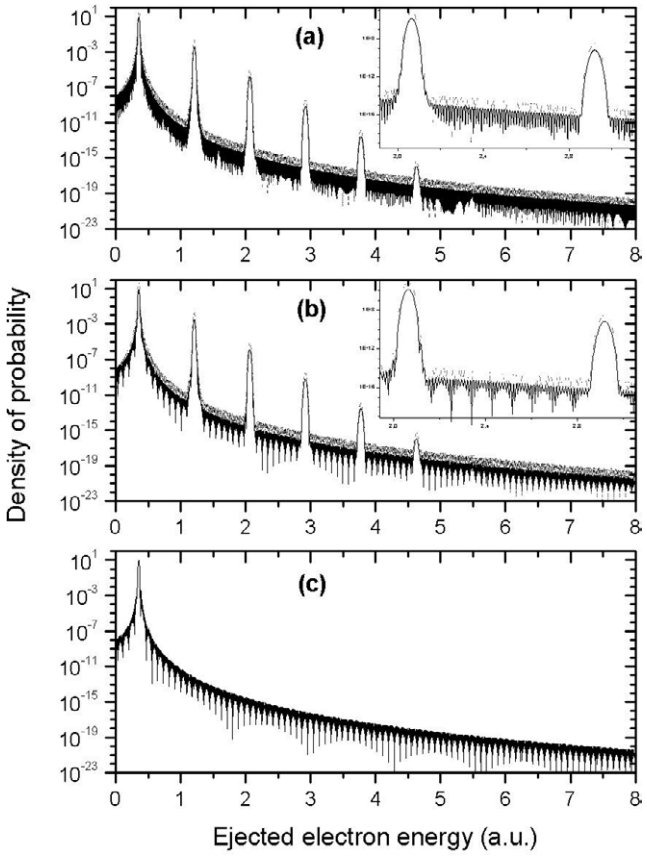

Figure 1. Ionization of $H(1s)$: electron distribution as a function of the energy of the ejected electron up to a maximum energy 8 au. Laser parameters are: photon energy $\omega = 0.855$, laser field amplitude $F = 0.05$ and pulse length $\tau = 500$. All quantities are given in atomic units. (a) Full line: TDSE; dotted line: SFA (length gauge). (b) Full line: Present CV2$^-$ spectrum; dotted line: SFA (length gauge) (c) First Born approximation spectrum. Inserts in figures (a) and (b) are close-up of 3rd and 4th peaks.

8 au. It is worth noting that, at variance with the figure 3(f) of paper [9], this new CV2$^-$ spectrum is quasi-identical to TDSE spectrum reported on figure 1(a) up to 8 au, thus showing the efficiency of the new time-integration procedure. Further, the present CV2$^-$ spectrum not only provides an accurate background in between multiphoton peaks, but it also permits to see the energy beyond which no more peak can show up. In figures 1(a) and (b), we also show the spectrum calculated within SFA. The length version of SFA has been evaluated by replacing the Coulomb continuum wavefunction in (32) by a plane wave. Although, we have verified that the ponderomotive potential U_p has no influence in the case analyzed here, all present calculations account for it. From the figure, we can see that SFA overestimate the background of the spectrum by a factor of 10. Multiphoton peaks predicted by SFA are also above TDSE ones, but by a smaller factor. Though it is not visible on the figure, we have verified that very close to threshold, TDSE exceeds SFA. This is ascribed to the absence of the Coulomb normalization factor giving rise to the cusp behavior for zero momentum [18]. It is clear that, by omitting the Coulomb interaction in the final channel, SFA leads to a significant loss of accuracy in the low energy part of the ATI spectrum. Since this conclusion is similar to experimental [5] and theoretical [7] findings in the IR domain, the conclusion holds from IR to UV wavelengths.

Figure 1(c) displays the spectrum predicted by B1. As expected, the one-photon ionization peak is very well described, whereas multi-photon peaks are not reproduced by this theory. Further, in agreement with the analysis made in section 3.1, B1 provides fairly accurate predictions of the spectrum background.

Now, electron distributions are obtained in [9] for a photon energy significantly higher than the ionization threshold. Thus, despite the laser spectral width, no resonance with bound intermediate state is expected to occur. Therefore, in view of the analysis made in section 3, the very good agreement between TDSE and CV2$^-$ is not a surprise. However, it has been shown [8, 9] that the standard CV2$^-$ cannot provide reliable predictions when $\omega < I_P$, i.e. when transitions through intermediate bound states may interference significantly with direct transitions. Again, it is no wonder in view of the analysis of section 3 that shows that direct transitions only are taken into account by the standard CV2$^-$ approach.

4.2. Justification of the modified CV2$^-$ approach

The MCV2$^-$ approach consists in introducing explicitly amplitudes of transitions through intermediate bound states that interfere with the standard CV2$^-$ amplitude [12]. Such a procedure, which showed to be very effective, is fully justified by the analysis made in section 3. Actually, amplitudes of transitions to the continuum through intermediate bound states $T_{ibf}^{(\mathrm{CV2}^-)}$ are obtained as follows: always in perturbation conditions, one integrates, over the pulse duration τ, the product of the amplitude $T_{ib}^{(I)}(t)$ to reach a given bound state b at a time t during the interaction, by the CV2$^-$ amplitude $T_{bf}^{(\mathrm{CV2}^-)}(t)$ to reach the continuum from the state b after t. Then one adds all $T_{ibf}^{(\mathrm{CV2}^-)}$ amplitudes to the standard CV2$^-$ one. Indeed, accurate phases are required for all amplitudes under consideration. Finally the MCV2$^-$ amplitude reads:

$$T_{if}^{(\mathrm{MCV2}^-)} = T_{if}^{(\mathrm{CV2}^-)} + \sum_b T_{ibf}^{(\mathrm{CV2}^-)}, \tag{38}$$

where one has:

$$T_{ibf}^{(\mathrm{CV2}^-)} = \int_0^\tau \mathrm{d}t\, T_{ib}^{(I)}(t)\, \exp\left\{\mathrm{i}\left(\frac{k^2}{2} - \varepsilon_j\right) t + \mathrm{i}\,\vec{k}\cdot\int_\tau^t \mathrm{d}t'\,\vec{A}^-(t')\right\} \vec{A}^-(t)\cdot\int \mathrm{d}\vec{r}\,\varphi_j(\vec{r})\exp\left[-\mathrm{i}\,\vec{A}^-(t)\cdot\vec{r}\right]\left[\mathrm{i}\,\vec{k} + \vec{\nabla}\right]\varphi_f^{-*}(\vec{r}). \tag{39}$$

It is worth noting that amplitudes $T_{ib}^{(I)}(0,t)$ may also be approximated by a CV2$^-$ approach adapted to the excitation process (see the next section). As a first test, only single-photon transitions to intermediate level b have been addressed in [12]. Therefore, a first-order perturbation calculation has been enough to get an accurate value of $T_{ib}^{(I)}(0,t)$. Indeed, by doing so, one does not expect to get reliable results for photon energies much lower than the energy required to reach the first excited state. However, for photon energies roughly higher than half the ionization potential I_P, very accurate and comprehensive electron spectra have been obtained [12].

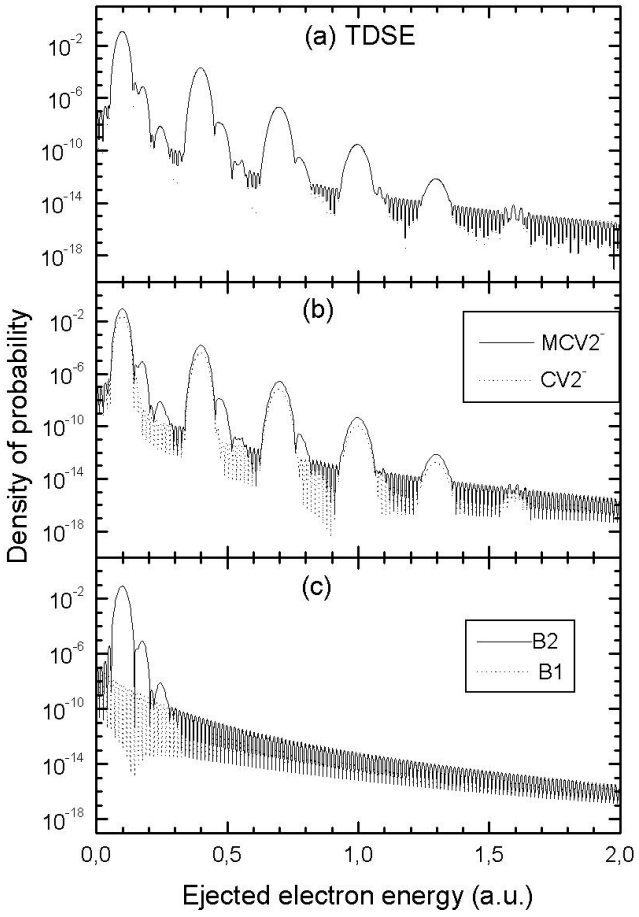

Figure 2. Ionization of $H(1s)$: electron distribution as a function of the energy of the ejected electron up to a maximum energy 2 au. Laser parameters are: photon energy $\omega = 0.3$, laser field amplitude $F = 0.02$ and pulse length $\tau = 837.758$ (40 cycles). All quantities are given in atomic units. (a) TDSE spectrum (b) Full line: MCV2$^-$spectra; dotted line: CV2$^-$. (c) First (dotted line) and second (full line) Born approximation spectra.

Here, some new spectra are analyzed in the light of the study of section 3.

4.3. Comparison between 2nd Born approximation and $MCV2^-$ approach

In figure 2(a), we show TDSE calculations for a photon energy smaller than the ionization threshold (($\omega = 0.3$ au) for a field amplitude $F = 0.02$ au. One observes clearly the appearance of a secondary peak structure. As analyzed in [12], these secondary peaks stem from multiphoton ionization through intermediate bound states due to the pulse bandwidth. The first ATI peak corresponds to a direct two-photon absorption from the ground state. As may be seen in figure 2(b), the CV2$^-$ theory is unable to reproduce the secondary peaks. On the contrary a MCV2$^-$ approach, that includes intermediate states up to 4*p*, brings significant improvement: it fully reproduces the details of the spectrum. Also shown in figure 2(c) is the second Born approximation (B2) calculated with the inclusion of bound states up to the principal quantum number $n = 20$. As expected, the first series of secondary peaks is well explained by B2, whereas no further peaks, neither main peaks, nor secondary peaks, can be reproduced by this theory. Therefore, MCV2$^-$ provides by far more information than the simple B2.

5. CV2$^-$ approach to laser-induced excitation of atoms

5.1. Multiphoton excitation $CV2^-$ amplitude

According to expression (16) and the remark made after expression (31), the transition amplitude CV2$^-$ that must be used for excitation reads:

$$T_{fi}^{\mathrm{CV2}^-} = -\mathrm{i}\int_0^\tau \mathrm{d}t\,\exp\left\{\mathrm{i}(\varepsilon_f-\varepsilon_i)t\right\}\int \mathrm{d}\vec{r}\,\bar{\varphi}_f^{\,*}(\vec{r}) \times \exp\left\{-\mathrm{i}\vec{A}^-(t)\cdot\vec{r}\right\}\vec{r}\cdot\vec{F}(t)\varphi_i(\vec{r}). \tag{40}$$

Here, we set $\vec{k} = \vec{0}$ because the final state is a bound state. To exhibit the consequences of ignoring intermediate resonances in standard CV2 approaches, we compare multiphoton excitation probabilities given by CV2$^-$ to the ones predicted by TDSE [14]. Hereafter, one considers excitation probabilities of $H(1s)$ atoms to $2p$ and $2s$ states as functions of the photon energy. As in previous papers, calculations are performed for laser pulses as defined in section 2 by expressions (6)–(8). As usual, one expects that transition probabilities will exhibit sharp peaks, hereafter referred to as principal peaks, when one has:

$$n\,\omega = \varepsilon_{2l} - \varepsilon_{1s}, \tag{41}$$

where n is an odd (resp. even) number of photons when the final state is $2p$ (resp. $2s$). Let us introduce:

$$\delta = \varepsilon_{2l} - \varepsilon_{1s} = 0.375\,\text{au}. \tag{42}$$

Thus, according to (41) and (42), a principal peak appears for the excitation of $2s$ or $2p$ states whenever the ratio δ/ω is an even or odd integer, respectively.

However, a spectral width of the laser pulse is the counterpart of the finite pulse duration. Therefore, photons whose energy is located on the wings of the laser spectrum may also contribute to excitation. Thus, peaks not satisfying equation (41) could also show up. In fact, these peaks would correspond to quasi-resonant transitions to intermediate states followed by transitions to the final state, that are induced by photons whose energy may be far from. Such resonant processes are not taken into account by standard CV2 treatments. In what follows, we consider 30-cycle laser pulses. Indeed, a fixed number of oscillations permits to keep the relative spectral width $\Delta\omega/\omega$ constant, whatever ω.

5.2. Multiphoton excitation of H(1s) to the 2p state

Excitation probabilities to the $2p$ state are reported for three values of the laser-field amplitude F: 10^{-4} au in figure 3(a), 10^{-3} au in figure 3(b) and 10^{-2} au in figure 3(c) corresponding to maximum intensities I of 3.51×10^{8}, 3.51×10^{10} and 3.51×10^{12}, respectively. As expected, the only peaks predicted by CV2$^-$ are principal peaks corresponding to the direct absorption of an odd number of photons (as long as

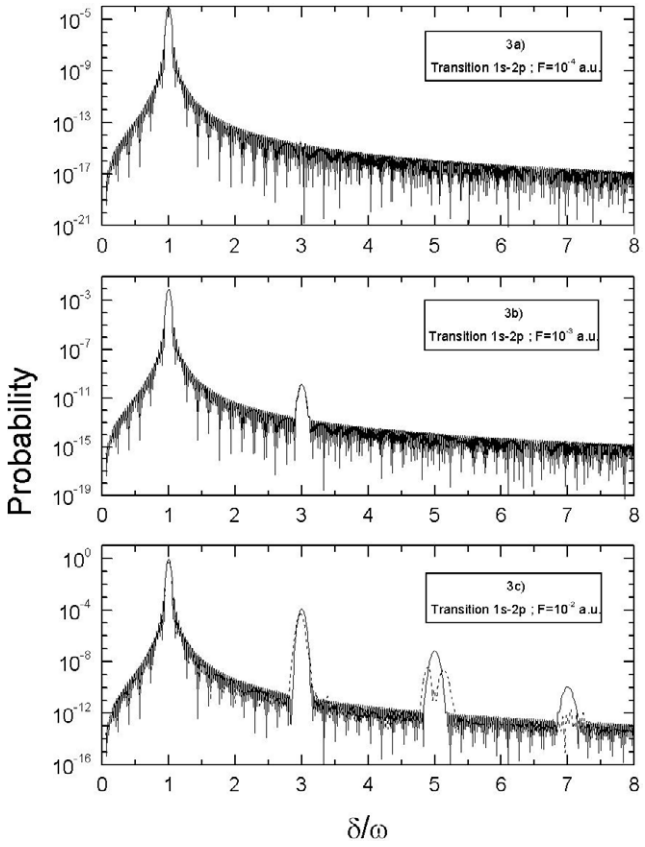

Figure 3. Probability to excite an $H(1s)$ atom to the state $2p$ by a 30 cycle-laser pulse as a function of the ratio where δ is the $1s$–$2p$ energygap and ω is the photon energy. The maximum amplitude of the electric field is: (a) $F = 10^{-4}$ (b) $F = 10^{-3}$ (c) $F = 10^{-2}$. Full line: CV2; dashed line: TDSE.

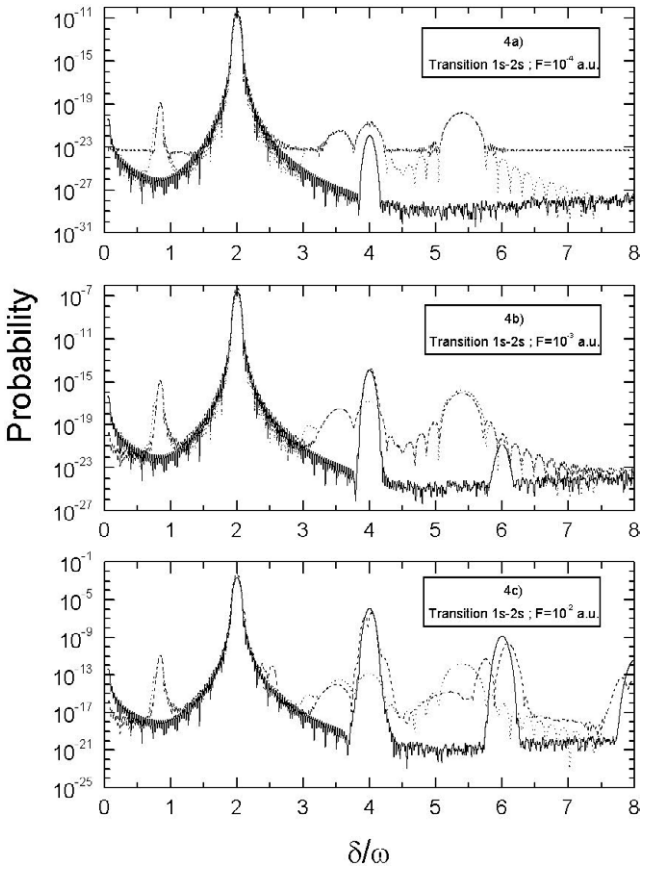

Figure 4. Same as figures 3(a)–(c), but for the excitation of the state $2s$. Dotted line: second Born approximation.

these peaks emerge above the background). Since transitions occur in a perturbation regime, the height of such peaks is $\propto I^n$, i.e. $\propto F^{2n}$ where n is the peak's order as defined in (41). It is exactly what can be checked for the 1st and 2nd peaks.

In all the figures, one sees that generally TDSE and CV2$^-$ calculations agree quite well. Single- and many-photon absorption peaks look very similar. On figure 3(a), the intensity is so weak that the first principal peak only shows up. On figure 3(c), a clear difference between TDSE and CV2$^-$ appears for the 3rd and 4th peaks that correspond to 5- and 7-photon absorption, respectively. The energy of photons for the 3rd peak is 0.075 au. Therefore, the absorption of an additional photon leads to the excitation of the state $3s$. Thus, the peak splitting, which appears in TDSE spectrum, might be an ac-Stark splitting (the so-called Autler–Townes splitting [19]) due to the strong dipolar coupling between $2p$ and $3s$ states. The efficiency of this one-photon depleting process is $\propto \sqrt{I}$. A similar splitting has been predicted recently in laser-induced positronium ionization [20]. Further, the absorption of a 7th photon leads to the continuum. These two later processes are fully taken into account in TDSE treatments whereas they are not in CV2$^-$. They are likely to lead to a significant depletion of the $2p$ level when both, the laser intensity and the $2p$ population are high enough. As a result, TDSE calculations let appear a sharp valley precisely at the expected maximum of the 3rd peak, as well as a broadening of this peak in figure 3(c). The situation is more complicated for the 4th peak since other couplings, which are more difficult to identify, might be involved in this case.

5.3. Multiphoton excitation of H(1s) to the 2s state

Excitation of the level $2s$ is quite different from the $2p$ one. Laser intensities under consideration are the same as in the previous section, but probabilities predicted by CV2 and TDSE, which are reported in figures 4(a)–(c), appear much smaller. As previously, the only peaks predicted by CV2$^-$ are principal peaks (as long as these peaks emerge above the background). However, they correspond to the direct absorption of an even number of photons in this case. Therefore, in a perturbation regime, the height of the nth peak is $\propto I^n$, i.e. $\propto F^{2n}$. It is exactly what one sees for all CV2 peaks on figures 4(a)–(c).

In figure 4(a), TDSE results are accurate only in the vicinity of the first principal peak, which results from a direct two-photon absorption. Due to the very weak probabilities, TDSE hardly reproduces the 'background' that is mainly made of the wings of this first peak. Indeed, this large broadening of the peak stems from the spectral laser width. Below $\delta/\omega = 4.2$ au, CV2$^-$ provide good predictions for the principal peaks only. However, CV2 height and TDSE height of the first principal peak differ roughly by a factor of 2. This discrepancy, which also appears in figures 4(b) and (c), indicates that again some indirect processes, which contribute to populate the state $2s$, are missing in CV2.

In all the figures 4(a)–(c), numerical round-off errors in time integration do not allow CV2 to well reproduce

the genuine background. Now, in figures 4(a) and (b), many substructures appear in TDSE results. Beyond the first principal peak, these substructures originate from complicated multiphoton processes that imply transient intermediate states excited by photons located in the wings of the laser spectral distribution.

More interestingly at $\delta/\omega \simeq 0.845$, TDSE calculations report a secondary peak that is present in the three figures. Its height varies as I^2 that is the signature of a two-photon process. Since the peak is clearly visible, one expects the energy of one of the two photons to be close to the centre of the laser-pulse spectrum. In this case, this energy is $\omega = 0.4438$ au. This value is very close to 0.4444 au that is the energy required to excite the level $3p$. Therefore, one may identify the peak at $\delta/\omega \simeq 0.845$ as a resonant one-photon excitation to the intermediate level $3p$ and a subsequent emission of a 0.0694 au photon, stimulated by the low-energy wing of the laser spectrum, that leads to the final level $2s$. This scenario is supported by second-order Born calculations that well reproduce TDSE predictions for this peak in all figures 4(a)–(c). Although such a two-photon process is not included in a standard CV2$^-$ treatment, it may be described using an approach similar to MCV2$^-$ [12]. In addition, we have performed similar calculations of 2s excitation using a Gaussian shape whose full width of half maximum (FWHM) is equal to the sine-square pulse one (cf (6) and (8)), with identical maximum intensities. In that case, the Gaussian pulse used in calculations has a longer duration and it results in a much smaller spectral laser width than the sine-square one. The figure 5 shows that, $2s$ excitation with the Gaussian pulse, the above-mentioned transitions through the $3p$ state do not appear anymore. This reveals the crucial role of the spectral laser width.

Trying to identify all processes that contribute to other secondary peaks appears almost hopeless. For example, the peak that shows up at $\delta/\omega \simeq 3.492$ au, i.e. $\omega = 0.1074$ au seems to stem also from a two-photon process if one compares its heights reported in figures 4(a) and (b). Such an interpretation is supported by the second-order Born calculations that well reproduce TDSE predictions for this peak, but only in these two figures. In fact, a two-photon transition to $2s$ is likely to be a 'direct' (non-resonant) transition. Indeed, a scenario similar to the previous case (peak at $\delta/\omega \simeq 0.845$) implies a 0.4444 au photon, i.e. a photon located very far in the high-energy wing of the laser spectrum, followed by a stimulated emission of a 0.0694 au photon. The energy of the first photon explains the small height of this peak. However, comparing the heights predicted by TDSE for this peak in figures 4(b) and (c) indicates that it is influenced by other multiphoton processes when the laser intensity increases. Indeed, the height ratio is no longer proportional to I^2. Moreover, second-order Born calculations no longer agree with TDSE predictions in figure 4(c).

6. Conclusions and perspectives

We have shown that, given a laser-induced electronic transition, a perturbation approach based on CV and called CV2 is able to give accurate excitation and ionization rates of atoms or molecules by short laser pulses as long as no intermediate resonant state interferes with a direct multiphoton transition. When intermediate resonant state are involved, the modified CV2$^-$ theory may be used [12]. Indeed, it has been stated that MCV2$^-$ compares well with B2 for two-photon transitions through intermediate bound-states where similar secondary peak structures appear. However, compared to the B2, MCV2$^-$ is a significant improvement. Indeed, TDSE numerical calculations show that MCV2$^-$ well predicts the whole structure of principal multi-photon peaks, as well as all series of secondary peaks. We have also shown that, like in recent theoretical [7] and experimental [5] findings in the IR domain, SFA leads to a considerable loss of accuracy in the low energy part of the ATI spectrum, thus enforcing the need to take into account the Coulomb interaction in the final states.

With respect to atomic multiphoton excitation, the theory CV2$^-$ also exhibits a multiphoton structure similar to the structure predicted by TDSE calculations. However, as expected from the analysis of section 3.1, CV2$^-$ cannot predict secondary structures stemming from excitation of transient intermediate states that may occur due to the laser spectral width. In this later case, an extension of the CV2 approach similar to MCV2$^-$ may be envisaged. Various CV approaches are particularly attractive because they are easy to implement with any atomic (many electrons) or molecular systems. Indeed, CV calculations require only a good description of a few wavefunctions (the initial and final states, and, eventually, a few intermediate states). Moreover, these approaches give a better understanding of the underlying physics since most significant processes may be identified explicitly.

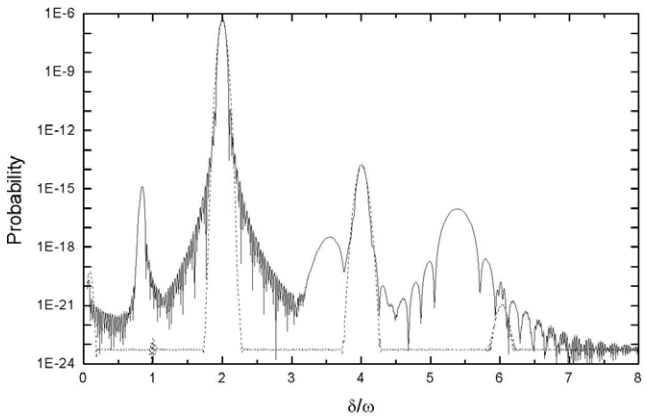

Figure 5. Probability to excite an $H(1s)$ atom to the state $2s$ by a $F = 10^{-3}$ and 30 cycle sine-squared and Gaussian laser pulse-shaped as a function of the ratio performed by TDSE. Full line: sine-squared; dashed line: Gaussian.

Acknowledgments

VDR acknowledges support by the Universidad de Buenos-Aires under grant X259, by the Consejo Nacional de Investigaciones Científicas y Técnicas (CONICET) under PIP 583 and the ANPCYT, PICT 20548. Calculations were performed with the M3PEC pole for parallel computing at the Université Bordeaux 1.

Appendix A. Background of the ionization spectrum given by the first Born approximation

Within the time interval $[0, \tau]$, the external field is:

$$\vec{F}(t) = F_0\,\vec{\lambda}\,\sin(\omega t+\varphi)\;\; f(t)$$
$$= \frac{F_0\,\vec{\lambda}}{2\mathrm{i}}\;\{\exp[\mathrm{i}\,(\omega t+\varphi)] - \exp[-\mathrm{i}\,(\omega t+\varphi)]\}\;\; f(t). \quad \text{(A.1)}$$

It is zero elsewhere. $\vec{\lambda}$ is the polarization and $f(t)$ describes the envelope of the pulse. Thus, the first Born transition amplitude reads:

$$T_{if}^{\mathrm{B1}} = -\mathrm{i}\int_{-\infty}^{+\infty}\mathrm{d}t\int\mathrm{d}\vec{r}\;\mathrm{e}^{\mathrm{i}\,\varepsilon_f\,t}\,\varphi_f^{-*}(\vec{r})\,\vec{r}\cdot\;\vec{F}(t)\,\mathrm{e}^{-\mathrm{i}\,\varepsilon_i\,t}\varphi_i(\vec{r})$$
$$= -\mathrm{i}\,F_0\int_0^{\tau}\mathrm{d}t\;\exp\left\{\mathrm{i}\left(\varepsilon_f-\varepsilon_i\right)t\right\}\,\sin(\omega t+\varphi)\;\,f(t)$$
$$\times\int\mathrm{d}\vec{r}\;\varphi_f^{-*}(\vec{r})\,\vec{r}\cdot\,\vec{\lambda}\,\varphi_i(\vec{r}). \quad \text{(A.2)}$$

Let us introduce:

$$\mathcal{F}_{ij} = -\mathrm{i}\,F_0\int_0^{\tau}\mathrm{d}t\;\exp\left\{\mathrm{i}\left(\varepsilon_f-\varepsilon_i\right)t\right\}\,\sin(\omega t+\varphi)\;\,f(t), \quad \text{(A.3)}$$

$$\vec{\lambda}\cdot\vec{r}_{ij} = \int\mathrm{d}\vec{r}\;\varphi_f^{-*}(\vec{r})\,\vec{r}\cdot\,\vec{\lambda}\,\varphi_i(\vec{r}). \quad \text{(A.4)}$$

Thus, one may write:

$$T_{if}^{B} = \mathcal{F}_{if}(\tau)\times\vec{\lambda}\cdot\vec{r}_{if}. \quad \text{(A.5)}$$

The time dependence is entirely contained in $\mathcal{F}_{ij}(\tau)$. One assumes $\varepsilon_f > \varepsilon_i$. Then, one defines:

$$\Delta\varepsilon = \varepsilon_f - \varepsilon_i > 0. \quad \text{(A.6)}$$

According to (A.1) one has now:

$$\mathcal{F}_{ij} = \frac{F_0}{2}\int_0^{\tau}\mathrm{d}t\;\exp\{\mathrm{i}\,\Delta\varepsilon\,t\}\,\{\exp[-\mathrm{i}(\omega t+\varphi)]$$
$$-\exp[\mathrm{i}(\omega t+\varphi)]\}\,f(t),$$
$$= \frac{F_0}{2}\int_0^{\tau}\mathrm{d}t\,\{\exp[\mathrm{i}(\Delta\varepsilon\;-\omega)t-\mathrm{i}\varphi]$$
$$-\exp[\mathrm{i}(\Delta\varepsilon\;+\omega)t+\mathrm{i}\varphi]\}\,f(t). \quad \text{(A.7)}$$

Since both ω and $\Delta\varepsilon$ are >0, the less oscillating term in (A.7) is the first one. Hence, one will deal now with:

$$\mathcal{F}_{ij} \approx \frac{F_0\mathrm{e}^{-\mathrm{i}\varphi}}{2}\int_0^{\tau}\mathrm{d}t\;\exp\{\mathrm{i}\;(\Delta\varepsilon-\omega)\;t\}\;\;f(t). \quad \text{(A.8)}$$

Then, we may address a few cases representative of a pulse *that contains many oscillations*.

Appendix A.1. Rectangular envelope

$$f(t) = 1. \quad \text{(A.9)}$$

In this case, one gets straightforward:

$$\mathcal{F}_{ij} \approx \frac{F_0\mathrm{e}^{-\mathrm{i}\varphi}}{2}\,\frac{\left[\exp\{\mathrm{i}(\Delta\varepsilon-\omega)\tau\}-1\right]}{\mathrm{i}\,(\Delta\varepsilon-\omega)}. \quad \text{(A.10)}$$

It may be transformed into:

$$\mathcal{F}_{ij} \approx \frac{F_0 e^{-\mathrm{i}\varphi}}{2\,\mathrm{i}\;(\Delta\varepsilon-\omega)}\;\exp\left\{\mathrm{i}\;(\Delta\varepsilon-\omega)\;\frac{\tau}{2}\right\}$$
$$\times\left[\exp\left\{\mathrm{i}\;(\Delta\varepsilon-\omega)\;\frac{\tau}{2}\right\}-\exp\left\{-\mathrm{i}\;(\Delta\varepsilon-\omega)\;\frac{\tau}{2}\right\}\right]$$
$$\approx \frac{F_0\mathrm{e}^{-\mathrm{i}\varphi}}{\Delta\varepsilon-\omega}\;\exp\left\{\mathrm{i}\;(\Delta\varepsilon-\omega)\;\frac{\tau}{2}\right\}\;\sin\left\{(\Delta\varepsilon-\omega)\;\frac{\tau}{2}\right\}. \quad \text{(A.11)}$$

This leads to the well-known result:

$$\left|\mathcal{F}_{ij}\right|^2 \approx F_0^2\,\frac{\sin^2\left\{(\Delta\varepsilon-\omega)\;\frac{\tau}{2}\right\}}{(\Delta\varepsilon-\omega)^2}. \quad \text{(A.12)}$$

Therefore, at a given position of the electron spectrum outside the peak, i.e. for a given value of $\Delta\varepsilon-\omega\neq 0$, $\left|\mathcal{F}_{ij}\right|^2$ oscillates with τ between 0 and a maximum value $F_0^2(\Delta\varepsilon-\omega)^2$, which does not depend on τ. However, the height of the peak (at the resonance, i.e. for $\Delta\varepsilon-\omega=0$) behaves as $F_0^2\,\tau^2/4$. As a result, the ratio of the height of a principal peak to the maximum height of the background at any energy, outside the peak itself, increases as τ^2.

Further, the zeros just before and just beyond the peak are given by:

$$(\Delta\varepsilon_{-1}-\omega)\;\frac{\tau}{2} = -\pi \Rightarrow \Delta\varepsilon_{-1} = -\frac{2\,\pi}{\tau}+\omega, \quad \text{(A.13}a\text{)}$$

$$(\Delta\varepsilon_{1}-\omega)\;\frac{\tau}{2} = +\pi \;\Rightarrow \Delta\varepsilon_{1} = \frac{2\,\pi}{\tau}+\omega. \quad \text{(A.13}b\text{)}$$

The distance between the two zeros is $4\pi/\tau$, thus showing that the peak width behaves as τ^{-1}. Let us define:

$$x = (\Delta\varepsilon-\omega)\;\frac{\tau}{2}. \quad \text{(A.14)}$$

Then, at half maximum, one has from (A.12) and (A.14):

$$\frac{F_0^2\,\tau^2}{8} = \frac{F_0^2\,\tau^2}{4}\,\frac{\sin^2 x}{x^2}. \quad \text{(A.15)}$$

The solution of (A.15) is:

$$|x| \simeq 1.3915574 \Rightarrow |\Delta\varepsilon-\omega| = \frac{2}{\tau}\times 1.3915574. \quad \text{(A.16)}$$

Therefore, the FWHM is twice the above value of $|\Delta\varepsilon-\omega|$, i.e.

$$\mathrm{FWHM} \simeq \frac{5.5662296}{\tau}. \quad \text{(A.17)}$$

Appendix A.2. Sine-square envelope

$$f(t) = \sin^2\left(\frac{\pi}{\tau}\,t\right) = \frac{1}{2}\left[1-\cos\left(\frac{2\,\pi}{\tau}t\right)\right]. \quad \text{(A 18)}$$

Again, neglecting the rapidly oscillating term in (A.7), one has:

$$\mathcal{F}_{ij} \approx \frac{\mathcal{F}_0\mathrm{e}^{-\mathrm{i}\varphi}}{4}\int_0^{\tau}\mathrm{d}t\;\exp\{\mathrm{i}\;(\Delta\varepsilon-\omega)\;t\}\;\left[1-\cos\left(\frac{2\,\pi\,t}{\tau}\right)\right]. \quad \text{(A.19)}$$

For the sake of simplicity, let us introduce:

$$\beta = \frac{2\,\pi}{\tau}, \quad \delta = \Delta\varepsilon - \omega. \tag{A.20}$$

Thus, one has:

$$\mathcal{F}_{ij} \approx \frac{F_0 \mathrm{e}^{-\mathrm{i}\varphi}}{4} \int_0^\tau \mathrm{d}t\, \mathrm{e}^{\mathrm{i}\delta t} \left[1 - \frac{\mathrm{e}^{\mathrm{i}\,\beta\,t} + \mathrm{e}^{-\mathrm{i}\,\beta\,t}}{2}\right]. \tag{A.21}$$

After an easy integration, one gets:

$$\mathcal{F}_{ij} \approx \frac{F_0 \mathrm{e}^{-\mathrm{i}\varphi}}{4} \left\{ \frac{\mathrm{e}^{\mathrm{i}\,\delta\,\tau} - 1}{\mathrm{i}\,\delta} - \frac{1}{2}\left[\frac{\mathrm{e}^{\mathrm{i}\,(\delta+\beta)\,\tau} - 1}{\mathrm{i}(\delta+\beta)} + \frac{\mathrm{e}^{\mathrm{i}\,(\delta-\beta)\,\tau} - 1}{\mathrm{i}(\delta-\beta)}\right]\right\}. \tag{A.22}$$

Then, from (A.20), one has $\beta\,\tau = 2\,\pi$, which leads to:

$$\begin{aligned}\mathcal{F}_{ij} &\approx \frac{F_0 \mathrm{e}^{-\mathrm{i}\varphi}}{4\,\mathrm{i}} \left(\mathrm{e}^{\mathrm{i}\,\delta\,\tau} - 1\right) \left\{ \frac{1}{\delta} - \frac{1}{2}\left[\frac{1}{(\delta+\beta)} + \frac{1}{(\delta-\beta)}\right]\right\} \\ &\simeq \frac{F_0 \mathrm{e}^{-\mathrm{i}\varphi}}{4\,\mathrm{i}} \left(\mathrm{e}^{\mathrm{i}\,\delta\,\tau} - 1\right) \left\{ \frac{-\beta^2}{\delta\left(\delta^2 - \beta^2\right)}\right\}. \end{aligned} \tag{A.23}$$

When τ becomes very large for a fixed value of δ, β becomes negligible compared to δ and one may write:

$$\mathcal{F}_{ij} \approx \frac{\mathrm{i}\,F_0\,\mathrm{e}^{-\mathrm{i}\varphi}}{4} \left(\mathrm{e}^{\mathrm{i}\,\delta\,\tau} - 1\right) \frac{\beta^2}{\delta^3} = \frac{-\,F_0\,\mathrm{e}^{\mathrm{i}\left(\frac{\delta\,\tau}{2} - \varphi\right)}}{2} \frac{\beta^2}{\delta^3} \sin\left(\frac{\delta\,\tau}{2}\right). \tag{A.24}$$

Finally, when $\delta \gg \beta$, one has:

$$|\mathcal{F}_{ij}|^2 \overrightarrow{\delta \gg \beta} \frac{F_0^2}{4} \frac{\beta^4}{\delta^6} \sin^2\left(\frac{\delta\tau}{2}\right) = \frac{4\pi^4 F_0^2}{(\Delta\varepsilon - \omega)^6} \frac{1}{\tau^4} \sin^2\left(\frac{\delta\tau}{2}\right). \tag{A.25}$$

Indeed, as it may be readily verified from (A.24), in the vicinity of the peak where $\delta \ll \beta$, one recovers the well-known expression obtained with a rectangular pulse, except a factor $\frac{1}{4}$ due to the shape of the sine square envelope. Thus, the amplitude of $\left|\mathcal{F}_{ij}\right|^2$ is $\propto \delta^{-2}$ close to the peak and $\propto \delta^{-6}\tau^{-4}$ far from it. Therefore, it does not depend on τ in the neighborhood of the peak.

Appendix B. Time-integration of the transition amplitude over the pulse duration

According to expressions (16)–(20) of the transition amplitude CV2, one has for a genuine laser pulse:

$$\begin{aligned} T_{fi}^{\mathrm{CV2^-}} = &-\mathrm{i}\int_0^\tau \mathrm{d}t \exp\left\{\mathrm{i}(\varepsilon_f - \varepsilon_i)t\right\} \exp\left\{\mathrm{i}\vec{k}\cdot\int_\tau^t \mathrm{d}t'\,\vec{A}^-(t')\right\} \\ &\times \left\{(\varepsilon_f - \varepsilon_i)t + \mathrm{i}\vec{k}\cdot\int_\tau^t \mathrm{d}t'\,\vec{A}^-(t')\right\} \\ &\times \int \mathrm{d}\vec{r}\,\varphi_f^{-*}(\vec{r}) \exp\{-\mathrm{i}\vec{A}^-(t)\cdot\vec{r}\}\varphi_i(\vec{r}). \end{aligned} \tag{B.1}$$

In (B1), the most rapidly oscillating factor is $\exp\{\mathrm{i}(\varepsilon_f - \varepsilon_i)t\}$. Hence, let us write $T_{\mathrm{fi}}^{\mathrm{CV2^-}}$ as:

$$T_{fi}^{\mathrm{CV2^-}} = \int_a^b \mathrm{d}t \exp\alpha\,(t)\,f\,(t), \tag{B.2}$$

where $a = 0$, $b = \tau$, $\alpha = \mathrm{i}(\varepsilon_f - \varepsilon_i)$ and $f\,(t)$ is the rest of the integrant. One divides the interval $a,\ b$ by means of $(n-1)$ intermediate pivots t_j where $j = 2,\ \ldots,\ n$. The extreme pivots are $t_1 = a$ and $t_{n+1} = b$. Then, one approaches $f\,(t)$ in each interval $[t_{j-1},\ t_{j+1}]$ by means of a parabola, i.e., one defines $(n-1)$ polynomials as follows:

$$g_j(t) = a_j t^2 + b_j t + c_j \quad \text{with} \quad j = 2, \ldots, n, \tag{B.3}$$

whose coefficients are determined by imposing:

$$g_j(t_{j-1}) = f\,(t_{j-1})\,; \quad g_j(t_j) = f\,(t_j)\,; \quad g_j(t_{j+1}) = f\,(t_{j+1}). \tag{B.4}$$

Thus, it is obvious that, except for $j = 2$, $g_j(t)$ shares the interval $[t_{j-1},\ t_j]$ with the previous polynomial $g_{j-1}(t)$. Similarly, except for $j = 2$, $g_j(t)$ shares the interval $[t_{j-1},\ t_{j+1}]$ with $g_{j+1}(t)$. Hence, to a very good approximation, one may write in the interval $[t_{j-1},\ t_j]$:

$$f\,(t) \simeq \tfrac{1}{2}\left[g_{j-1}(t) + g_j(t)\right] \quad \text{with} \quad 2 \leqslant j \leqslant n. \tag{B.5}$$

Therefore, the integral in (B.2) takes the form:

$$\begin{aligned} T_{fi}^{\mathrm{CV2^-}} \simeq \frac{1}{2}\Bigg\{ &\int_{t_1}^{t_2} \mathrm{d}t\,\mathrm{e}^{\alpha\,t}\,g_2(t) + \sum_{j=2}^{n} \int_{t_{j-1}}^{t_{j+1}} \mathrm{d}t\,\mathrm{e}^{\alpha\,t}\,g_j(t) \\ &+ \int_{t_n}^{t_{n+1}} \mathrm{d}t\,\mathrm{e}^{\alpha\,t}\,g_n(t)\Bigg\}. \end{aligned} \tag{B.6}$$

The two integrals in the intervals $[t_1,\ t_2]$ and $[t_n,\ t_{n+1}]$ must be introduced because the sum over j contains only one integration in these intervals whereas two integrations are performed with $g_j(t)$ and $g_{j+1}(t)$ in all other intervals $[t_j,\ t_{j+12}]$. The integrals in (B.6) are carried out analytically. A fast computing code has been written for equidistant pivots. The accuracy of the outcome may be checked easily by increasing the number of pivots. For example, the spectrum in figure 1(b), which is made up of 2000 points, is obtained in less than 1 min on a 1 GHz PC with $n = 100$ for the time integration.

Appendix C. Comparison between BPS and CV2$^-$ perturbation expansion

Let us come back to the two-photon amplitude (30) without the electron displacement term and using (2(a) and (b)):

$$T_{fi}^{\mathrm{CV2^-}(2)} = (-\mathrm{i}\,\alpha)^2 \int_0^\tau \mathrm{d}t \int \mathrm{d}\vec{r}\,\phi_f^{-*}(\vec{r},t)\vec{r}\cdot\vec{A}_0^-(t)\vec{r}\cdot\vec{F}_0(t)\phi_i(\vec{r},t). \tag{C.1}$$

Substituting $\vec{r}\cdot\vec{F}_0(t)$ for $V(t)$ in the corresponding second-order term of the BPS (23), one gets:

$$\begin{aligned} T_{fi}^{(2)} = &(-\mathrm{i}\,\alpha)^2 \int_0^\tau \mathrm{d}t \int_0^t \mathrm{d}t' \int \mathrm{d}\vec{r}\,\phi_f^{-*}(\vec{r},t)\,\vec{r}\cdot\vec{F}_0(t) \\ &\times \sum_j \phi_j(\vec{r},t) \int \mathrm{d}\vec{r}'\phi_j^*(\vec{r}',t')\,\vec{r}'\cdot\vec{F}_0(t')\,\phi_i(\vec{r}',t'). \end{aligned} \tag{C.2}$$

In the integrant, let us look at the factor:

$$\Gamma_{ji}(t) = \int_0^t \mathrm{d}t' \int \mathrm{d}\vec{r}'\phi_j^*(\vec{r}',t')\,\vec{r}'\cdot\vec{F}_0(t')\,\phi_i(\vec{r}',t'). \tag{C.3}$$

One defines:

$$\vec{F}_0(t') = \hat{\lambda}\, F_0(t'), \tag{C.4}$$

$$D_{ji}(t') = \int \mathrm{d}\vec{r}\, \phi_j^*(\vec{r},t')\, \vec{r}\cdot\hat{\lambda}\, \phi_i(\vec{r}\,,t') = \langle \phi_j(t')|\ \vec{r}\cdot\hat{\lambda}\ |\phi_i(t')\rangle. \tag{C.5}$$

Thus, one has:

$$\Gamma_{ji}(t) = \int_0^t \mathrm{d}t'\, F_0(t')\, D_{ji}(t'). \tag{C.6}$$

Let us introduce:

$$\vec{A}_0(t) = -\int_0^t \mathrm{d}t'\, F_0(t'). \tag{C.7}$$

An integration by parts of (C.3) leads to :

$$\Gamma_{ji}(t) = \left[-A_0(t')\, D_{ji}(t')\right]_0^t + \int_0^t \mathrm{d}t'\, A_0(t')\, \frac{\mathrm{d}}{\mathrm{d}t'} D_{ji}(t'). \tag{C.8}$$

Since $\vec{A}_0(0) = \vec{0}$, one has:

$$\Gamma_{ji}(t) = -A_0(t)\, D_{ji}(t) + \int_0^t \mathrm{d}t'\, A_0(t')\, \frac{\mathrm{d}}{\mathrm{d}t'} D_{ji}(t')\,. \tag{C.9}$$

Let us examine the 2nd term in the rhs of (C.9):

$$\frac{\mathrm{d}}{\mathrm{d}t} D_{ji}(t) = \langle \frac{\mathrm{d}}{\mathrm{d}t}\phi_j(t)|\ \vec{r}\cdot\hat{\lambda}\ |\phi_i(t)\rangle + \langle \phi_j(t)|\ \vec{r}\cdot\hat{\lambda}\ |\frac{\mathrm{d}}{\mathrm{d}t}\phi_i(t)\rangle. \tag{C.10}$$

where:

$$|\frac{\mathrm{d}}{\mathrm{d}t}\phi_i(t)\rangle = \frac{1}{\mathrm{i}}\left(\mathrm{i}\frac{\mathrm{d}}{\mathrm{d}t}\right)|\phi_i(t)\rangle = \frac{1}{\mathrm{i}}\, H_0\, |\phi_i(t)\rangle = \frac{\varepsilon_i}{\mathrm{i}}\ |\phi_i(t)\rangle\,. \tag{C.11a}$$

From (C.11*a*) the time derivative of the bra is:

$$\langle \frac{\mathrm{d}}{\mathrm{d}t}\phi_j(t)| = -\frac{\varepsilon_j}{\mathrm{i}}\ \langle \phi_j(t)|\,. \tag{C.11b}$$

Thus, one has:

$$\frac{\mathrm{d}}{\mathrm{d}t} D_{ji}(t) = \frac{\varepsilon_i - \varepsilon_j}{\mathrm{i}}\ \langle \phi_j(t)|\ \vec{r}\cdot\hat{\lambda}\ |\phi_i(t)\rangle = \frac{\varepsilon_i - \varepsilon_j}{\mathrm{i}}\ D_{ji}(t). \tag{C.12}$$

Let us integrate equation (C.12). One gets:

$$D_{ji}(t) = D_{ji}(0)\ \exp\left[\mathrm{i}\left(\varepsilon_j - \varepsilon_i\right)t\right], \tag{C.13}$$

where $D_{ji}(0)$ is the standard dipolar matrix element:

$$D_{ji}(0) = \int \mathrm{d}\vec{r}\varphi_j^*(\vec{r})\, \vec{r}\cdot\hat{\lambda}\, \varphi_i(\vec{r}). \tag{C.14}$$

Therefore $\Gamma_{ji}(t)$ now reads:

$$\Gamma_{ji}(t) = -A_0(t)\, D_{ji}(t) + \mathrm{i}(\varepsilon_j - \varepsilon_i) D_{ji}(0) \times \int_0^t \mathrm{d}t'\, A_0(t')\ \exp\left[\mathrm{i}\left(\varepsilon_j - \varepsilon_i\right)t'\right]. \tag{C.15}$$

The first term in the rhs of (C.15) corresponds to the second order of the CV2$^-$ perturbation series. In the 2nd term, $A_0(t')$ is oscillating mainly with the pulsation ω. As a result, the contribution of this 2nd term is significant only when the whole integrant does not oscillate (or is a slowly varying function of t', i.e. when one has:

$$\omega \simeq \left|\varepsilon_j - \varepsilon_i\right|. \tag{C.16}$$

The equation (C.16) corresponds to a resonance. The contribution of such a resonance is never taken into account in CV2$^-$ transition amplitudes as it will be shown hereafter. The definition (C.6) permits to write the expression (C.2) as:

$$T_{fi}^{(2)} = (-\mathrm{i}\,\alpha)^2 \int_0^\tau \mathrm{d}t\, F_0(t) \sum_j D_{fj}(t)\, \Gamma_{ji}(t). \tag{C.17}$$

Therefore, introducing (C.15) in (C.17), the 2nd order of the BPS is:

$$T_{fi}^{(2)} = -(-\mathrm{i}\,\alpha)^2 \int_0^\tau \mathrm{d}t\, F_0(t) \sum_j D_{fj}(t)\, A_0(t)\, D_{ji}(t) + (-\mathrm{i}\,\alpha)^2\, \mathrm{i}(\varepsilon_j - \varepsilon_i) \int_0^\tau \mathrm{d}t\, F_0(t) \sum_j D_{fj}(t)\, D_{ji}(0) \times \int_0^t \mathrm{d}t'\, A_0(t')\ \exp\left\{\mathrm{i}\left(\varepsilon_j - \varepsilon_i\right)t'\right\}, \tag{C.18}$$

while the second order of the CV2$^-$ perturbation series is:

$$T_{fi}^{\mathrm{CV2}^-\,(2)} = (-\mathrm{i}\,\alpha)^2 \int_0^\tau \mathrm{d}t \int \mathrm{d}\vec{r}\, \phi_f^{-*}(\vec{r},t)\vec{r}\ \cdot\ \vec{A}_0^-(t) \times \int \mathrm{d}\vec{r}' \sum_j \varphi_j(\vec{r})\, \varphi_j^*(\vec{r}')\, \vec{r}'\ \cdot\ \vec{F}_0(t)\, \phi_i(\vec{r}',t)$$

$$= (-\mathrm{i}\,\alpha)^2 \int_0^\tau \mathrm{d}t\, A_0^-(t) \sum_j D_{fj}(t)\, F_0(t)\, D_{ji}(t), \tag{C.19a}$$

$$= (-\mathrm{i}\,\alpha)^2 \int_0^\tau \mathrm{d}t\, F_0(t) \sum_j D_{fj}(t)\, A_0^-(t)\, D_{ji}(t). \tag{C.19b}$$

The definition (C.5) has been used to get expression (C.19*a*). Since $A_0^-(t) = A_0(t)$, the expression (C.19*b*) is identical to the first term in the rhs of (C.18), apart from a factor (-1). Indeed, this factor does not change predictions related to two-photon transitions. To shed more light on what is missing in standard CV2 approaches, let us write (C.19*b*) as:

$$T_{fi}^{\mathrm{CV2}^-\,(2)} = (-\mathrm{i}\,\alpha)^2 \int_0^\tau \mathrm{d}t\, F_0(t) \sum_j D_{fj}(t) \times \int_0^t \mathrm{d}t'\, \delta\left(t'-t\right) A_0^-(t')\, D_{ji}(t'). \tag{C.20}$$

Then, let us introduce:

$$\tilde{\Gamma}_{ji}(t) = \int_0^t \mathrm{d}t' \delta(t'-t) A_0(t') D_{ji}(t') = -D_{ji}(t) \int_0^t \mathrm{d}t'\, F_0(t'). \tag{C.21}$$

$\tilde{\Gamma}_{ji}(t)$ resembles $\Gamma_{ji}(t)$, except that $D_{ji}(t)$ is outside the time integral (see expression (C.6)). Thus, one has:

$$T_{fi}^{\mathrm{CV2}^-\,(2)} = (-\mathrm{i}\alpha)^2 \int_0^\tau \mathrm{d}t\, F_0(t) \sum_j D_{fj}(t)\, \tilde{\Gamma}_{ji}(t). \tag{C.22}$$

References

[1] Keldysh L V 1965 *Sov. Phys.—JETP* **20** 1307
Faisal F H M 1973 *J. Phys. B: At. Mol. Opt. Phys.* **6** L89
Reiss H 1980 *Phys. Rev.* A **22** 17
Becker A and Faisal F H M 2005 *J. Phys. B: At. Mol. Opt. Phys.* **38** R1–56

[2] Lewenstein M, Balcou P, Ivanov M Y, L'Huillier A and Corkum P B 1994 *Phys. Rev.* A **49** 2117–32

[3] Gribakin G F and Kuchiev M Y 1997 *Phys. Rev.* A **55** 3760–71
Bauer D, Milosevic D B and Becker W 2006 *Phys. Rev.* A **72** 023415–1

[4] Milosevic D B and Ehlotzky F 2003 *Adv. At. Mol. Phys.* **49** 373

[5] Rudenko A, Zrost K, Ergler Th, Voitkiv A B, Najjari B, de Jesus V L B, Feuerstein B, Schröter C D, Moshammer R and Ullrich J 2005 *J. Phys. B: At. Mol. Opt. Phys.* **38** L191–8

[6] Basile S, Trombetta F and Ferrante G 2005 *Phys. Rev. Lett.* **61** 2435

[7] Bauer D, Milosevic D B and Becker W 2006 *J. Mod. Optics* **53** 135–47

[8] Duchateau G, Cormier E and Gayet R 2003 *J. Mod. Optics* **50** 331

[9] Duchateau G, Cormier E and Gayet R 2002 *Phys. Rev.* A **66** 023412

[10] Jain M and Tzoar N 1978 *Phys. Rev.* A **18** 538–45

[11] Gayet R 2005 *J. Phys. B: At. Mol. Opt. Phys.* **38** 3905–16

[12] Rodriguez V D, Cormier E and Gayet R 2004 *Phys. Rev.* A **69** 053402

[13] Paul P M, Toma E S, Breger P, Mullot G, Augé F, Balcou P, Muller H G and Agostini P 2001 *Sciences* **292** 1689–92

[14] Cormier E and Lambropoulos P 1997 *J. Phys. B: At. Mol. Opt. Phys.* **30** 77–91

[15] Nordsieck A 1954 *Phys. Rev.* **93** 785

[16] Pan L, Armstrong L and Eberly J H 1986 *J. Opt. Soc. Am.* B **3** 1319

[17] Messiah A 1970 *Quantum Mechanics* vol II (Amsterdam: North Holland) chapter XVII p 724–28

[18] Fiol J, Barrachina R O and Rodríguez V D 2002 *J. Phys. B: At. Mol. Opt. Phys.* **35** 149

[19] Autler S H and Townes C H 1955 *Phys. Rev.* **100** 703

[20] Rodriguez V D 2006 *Nucl. Instrum. Methods Phys. Res.* **247** 105–10